Molecular Microbiology (2019) 112(6), 1814–1830

doi:10.1111/mmi.14395
First published online 9 October 2019

Two hybrid histidine kinases, TcsB and the phytochrome FphA, are involved in temperature sensing in *Aspergillus nidulans*

Zhenzhong Yu,[1,3,#] Arin Ali,[1,#] Olumuyiwa Ayokunle Igbalajobi,[1] Christian Streng,[1] Kai Leister,[1] Norbert Krauß,[2] Tilman Lamparter[2*] and Reinhard Fischer [1*]

[1] *Institute for Applied Biosciences, Department of Microbiology, Karlsruhe Institute of Technology (KIT) - South Campus, Fritz-Haber-Weg 4, Karlsruhe D-76131, Germany.*

[2] *Botanical Institute, Karlsruhe Institute of Technology (KIT) - South Campus, Karlsruhe D-76131, Germany.*

[3] *Jiangsu Provincial Key Laboratory of Organic Solid Waste Utilization, College of Resources and Environmental Sciences, Nanjing Agricultural University, Nanjing 210095, China.*

Summary

The adaptation of microorganisms to different temperatures is an advantage in habitats with steadily changing conditions and raises the question about temperature sensing. Here we show that in the filamentous fungus *Aspergillus nidulans,* the hybrid histidine kinase TcsB and phytochrome are involved in temperature-induced gene transcription. Temperature-activated phytochrome fed the signal into the HOG MAP kinase pathway. There is evidence that the photoreceptor phytochrome fulfills a temperature sensory role in plants and bacteria. The effects in plants are based on dark reversion from the active form of phytochrome, Pfr, to the inactive form, Pr. Elevated temperature leads to higher dark reversion rates, and hence, temperature sensing depends on light. In *A. nidulans* and in *Alternaria alternata,* the temperature response was light-independent. In order to understand the primary temperature response of phytochrome, we performed spectral analyses of recombinant FphA from both fungi. Spectral properties after heat stress resembled the spectrum of free biliverdin, suggesting conformational changes and a softening of the binding pocket of phytochrome, possibly mimicking photoactivation. We propose a novel function for fungal phytochrome as temperature sensor.

Accepted 22 September, 2019. *For correspondence. E-mail tilman.lamparter@kit.edu (T. L.); Tel. (+49) 721-608-45441; Fax (+49) 721-608-44193, reinhard.fischer@KIT.edu (R. F.); Tel. (+49) 721-6084-4630; Fax (+49) 721-6084-4509. #These authors contributed equally to this work.

Introduction

Temperature is an important factor which frequently changes in the environment, and microorganisms should be able to adapt accordingly. Temperature may affect many properties of a living cell, such as the nucleic acid structure, membrane fluidity, or enzymatic activities and these changes may drastically affect the fitness of a cell in general. It is well established that sudden drastic temperature increases in the ambient environment lead to the so-called heat-shock response, a quick reaction to reduce the damage caused by high temperatures (Gomez-Pastor *et al.*, 2018). However, a response to smaller changes in temperature may also be very important for survival, and therefore, adaptation processes are installed in many organisms. In bacteria with alternative free-living and pathogenic life styles, the higher temperature in warm-blooded animals is a reliable parameter to indicate host residence (Loh *et al.*, 2018). This new environment requires many changes in the pathogen to cope with changes in nutrient availability, host defense mechanisms or to enable quorum sensing to determine the population size.

Pathogenic fungi with a free-living and a pathogenic life style face the same problem as pathogenic bacteria. Excellent examples to show the importance of adaptations to the human host temperature as compared to growth outside a host are *Aspergillus fumigatus* and *Candida albicans* (O'Meara and Cowen, 2014; van de Veerdonk *et al.*, 2017). There is some evidence in *A. fumigatus* that the high-osmolarity glycerol mitogen-activated protein kinase (HOG-MAPK) pathway is required for temperature sensing (Ji *et al.*, 2012), and the global regulator LaeA and the transcription factor VeA appear to be important for some temperature responses (Lind *et al.*, 2016). Temperature changes can not only trigger physiological but also morphological changes. *Penicillium marneffei,* for instance, grows well in soil at low temperature with

filamentous hyphae and reproduces with aerial conidiophores (Borneman *et al*., 2000). Upon infection of animals, it undergoes dimorphic switching toward a fission yeast life style. The effect can be achieved in the laboratory solely by growing the fungus at different temperatures (Borneman *et al*., 2000). In another dimorphic fungus, *Blastomyces dermatitidis*, the dimorphism-regulating histidine kinase Drk1, an orthologue of the *Saccharomyces cerevisiae* hybrid histidine kinase Sln1 was discovered in a genetic screen (Nemecek *et al*., 2006). Whether temperature or another environmental cue was sensed by Drk1 remained open. In *S. cerevisiae,* the high-osmolarity glycerol (HOG) pathway can be activated under hyperosmotic stress by at least two upstream branches, the Sln1 and the Sho1 branch. Whereas Sln1 is specific for osmo-stress sensing, Sho1 is involved in osmo- and in heat-stress sensing (Winkler *et al*., 2002; Engelberg *et al*., 2014). *C. albicans* also undergoes morphological changes in the host, temperature is an important environmental signal, and the HOG pathway is the main pathway to adapt to environmental stresses (Liang *et al*., 2014; O'Meara and Cowen, 2014; Erwig and Gow, 2016; da Silva Dantas *et al*., 2016).

Temperature sensing is advantageous for soil-borne saprotrophic fungi as well. These fungi may experience drastic temperature changes throughout a day accompanied by drought and other stresses (Rodriguez-Romero *et al*., 2010; Yu and Fischer, 2019). Small temperature increases in the morning indicate the upcoming, "stressful" day. Such an alerting function has been proposed for light, and it was shown that the light responses in *A. nidulans*, *A. alternata* and *Trichoderma atroviride* share the central stress pathway, the HOG pathway, or are linked to it (Fuller *et al*., 2015; Esquivel-Naranjo *et al*., 2016; Fischer *et al*., 2016; Yu *et al*., 2016; Igbalajobi *et al*., 2019; Yu and Fischer, 2019). Temperature sensing hence allows stress adaptations underground in the dark. The described reactions on temperature changes raise the question about the underlying molecular temperature-sensing mechanisms. In *A. nidulans,* an orthologue of Sln1 was identified and named TcsB (Furukawa *et al*., 2002). The protein could complement the osmosensing defects in a *sln1* mutant of *S. cerevisiae* and activated the HOG pathway. However, deletion of *tcsB* in *A. nidulans* did not cause any significant phenotypic changes and a role in temperature sensing had not been tested.

In bacteria, ambient temperature changes may be sensed by certain RNA molecules with temperature-dependent translational control (Loh *et al*., 2018). Temperature increases cause changes in the tertiary structure of the RNA molecule followed by ribosome binding and translation. The produced protein may control the expression of virulence factors. Because the RNA molecule acting as thermometer is already synthesized and present in the cell, the physiological response can be very quick. Recent studies in plants revealed the possibility that phytochrome, the red-light photoreceptor in plants, is involved in temperature sensing. It was shown that the *Arabidopsis thaliana* phytochrome B (PhyB) binds to target genes in a temperature-dependent manner (Jung *et al*., 2016; Rockwell and Lagarias, 2017). Temperature modulates the dark reversion rate of phytochrome and thus changes the balance between Pr and Pfr in light (Legris *et al*., 2016; Casal and Qüesta, 2018; Sakamoto and Kimura, 2018; Park and Park, 2019; Qiu *et al*., 2019). Further evidence for phytochrome as temperature sensor comes from studies in bacteria. Conjugation of the soil bacterium *Agrobacterium fabrum* is regulated by phytochrome and temperature, and both regulations are lost in phytochrome knockout mutants (Bai *et al*., 2016). Furthermore, temperature effects on spectral properties and enzyme activities of bacterial phytochromes were shown (Njimona *et al*., 2014). Phytochrome is also present in many fungi, with the exception of *Saccharomyces cerevisiae* and some others, although clear red-light photo effects have only been demonstrated in a few fungi so far (Froehlich *et al*., 2005; Fischer *et al*., 2016; Wang *et al*., 2016; Schumacher, 2017; Igbalajobi *et al*., 2019). In *A. nidulans* and *A. alternata*, phytochrome controls morphological processes and physiological pathways such as the formation of alternariol (Blumenstein *et al*., 2005; Fischer *et al*., 2016; Igbalajobi *et al*., 2019; Yu and Fischer, 2019; Wenderoth *et al*., 2019). Here we discovered that the *A. nidulans* TcsB hybrid histidine kinase is involved in heat-stress sensing and that *A. nidulans* and *A. alternata* phytochromes serve dual functions as light sensor and possibly as light-independent thermometer.

Results

The A. nidulans *hybrid histidine kinase* TcsB *is involved in temperature sensing*

The molecular biology of light sensing and signaling has been investigated with the help of several light-regulated genes, two of which are *ccgA* and a close homologue thereof, *ccgB* (Ruger-Herreros *et al*., 2011). We found that both genes were highly upregulated in mycelium of *A. nidulans* after a temperature shift from 28 to 42°C in the dark. Because there is some evidence that a *S. cerevisiae* Sln1 hybrid histidine kinase orthologue, Drk1, is involved in temperature sensing in dimorphic fungi, we tested if the *A. nidulans* orthologue, TcsB, fulfills such a function (Furukawa *et al*., 2002; Nemecek *et al*., 2006). In *S. cerevisiae,* Sln1 is not required for heat-stress sensing. In order to test if the hybrid histidine kinase is involved in heat sensing in *A. nidulans*, we deleted *tcsB*. Heat-stress induction of the two marker genes, *ccgA* and *ccgB*, was

greatly reduced in the Δ*tcsB*-deletion strain as compared to wild type (Fig. 1). This situation hence resembles the situation in *B. dermatitidis.*

In order to test if a *S. cerevisiae* Sho1 orthologue, ShoA, could also be involved in heat-stress sensing in *A. nidulans*, a *shoA*-deletion strain was constructed and analyzed for temperature-dependent gene activation (Winkler *et al.*, 2002; Engelberg *et al.*, 2014). The transcription of both genes, *ccgA* and *ccgB,* was still stimulated by temperature as in wild type (Suppl. Fig. S1). This result clearly shows that temperature sensing is independent of ShoA. The roles of the Sln1 and Sho1 orthologues in temperature sensing in *A. nidulans* are thus opposite to their roles in *S. cerevisiae.*

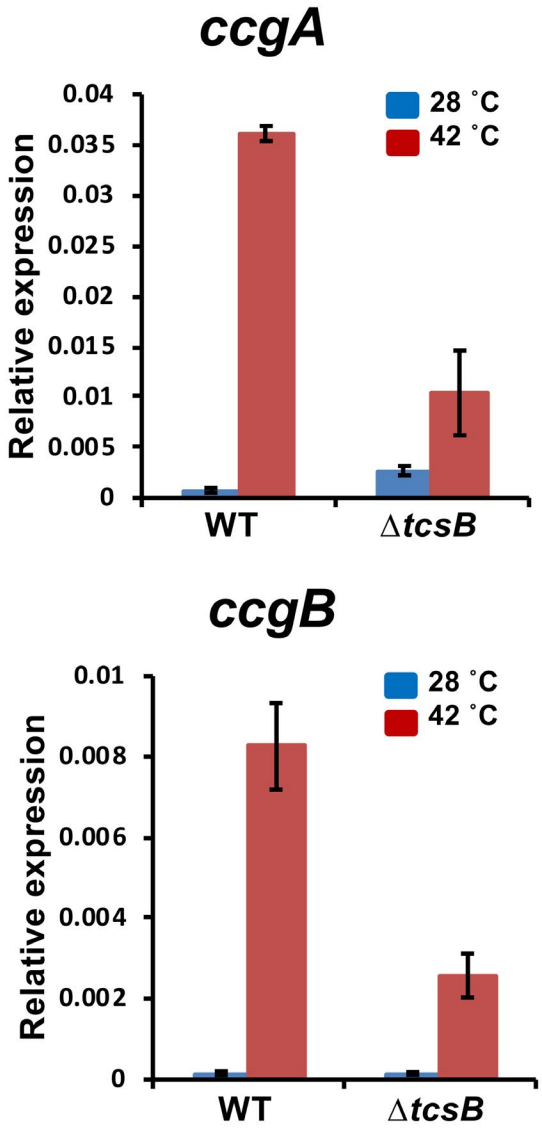

Fig. 1. Expression analysis of *ccgA* and *ccgB* in wild-type (WT) and a Δ*tcsB*-deletion strain. Spores of wild-type (WT) (SJR2) and of the Δ*tcsB*-deletion strain (SZY72) were cultured on the surface of supplemented minimal medium at 28°C for 18 h in the dark. The mycelia were then transferred onto the surface of fresh minimal medium pre-warmed to 28 or 42°C and incubated for 10 min in the dark. Then, the mycelia were frozen immediately in liquid nitrogen followed by RNA isolation. The expression levels of *ccgA* and *ccgB* were normalized to the histone *h2b* gene. The bars present mean values ± SD of three biological replicates.

The hybrid histidine kinase phytochrome as a novel temperature sensor

Previously, we constructed an *A. nidulans* nucleotide–auxotrophic strain (parent strain) where a nutritional marker gene, *pyr4*, was placed under the control of the light-regulated promoter *conJ* (Yu *et al.*, 2016). The strain grows well in media supplemented with uracil and uridine independent of light but grows on minimal medium only when exposed to light. We used this strain to isolate *blind* mutants (UV light as mutagen), which did not grow even under light incubation but only after supplementation of the medium with uracil and uridine. This led to the discovery of the involvement of the SakA stress- and osmosensing pathway in light sensing in *A. nidulans* (Yu *et al.*, 2016). One of the isolated mutants had a defect in phytochrome itself. Here, we observed that growth of the parent strain on minimal medium is not only stimulated by light but also by temperature, suggesting that the *conJ* promoter is also under temperature control (Fig. 2). Measurements of the transcript levels of *conJ* before and after heat stress confirmed this induction (Suppl. Fig. S2). In order to test for a possible role of phytochrome and the SakA pathway in temperature sensing of *A. nidulans*, we tested the phytochrome mutant isolated in the mutagenesis experiment and the *sakA* mutant for their ability to respond to higher temperatures. Both mutants grew very slowly at 42°C in comparison to the corresponding re-complemented strains or to the wild type. Although hyphal growth of the phytochrome mutant re-complemented with a phytochrome wild-type copy was restored, sporulation was affected. This shows that the phytochrome mutant strain harbors additional mutations after the UV mutagenesis, which is also obvious in the colonies grown on agar plates supplemented with uracil and uridine in the dark. Nevertheless, the results provided first indications that phytochrome and the HOG pathway are involved in temperature sensing in *A. nidulans*. In terms of light sensing in *A. nidulans*, phytochrome is regarded as the first protein in the signal transduction chain and uses the HOG pathway to activate downstream genes such as *conJ*. Therefore, we anticipated that phytochrome is also the first protein in the temperature signal transduction chain, that is, it functions as *thermometer*. Clearly, in *A. nidulans* light is not required for temperature sensing via phytochrome (Fig. 2). Because incubation of *A. nidulans* at different temperatures causes changes in development, we tested if phytochrome had any effect on such developmental decisions at different temperatures (Suppl. Fig. S3). We found that at 28 and 37°C cleistothecia

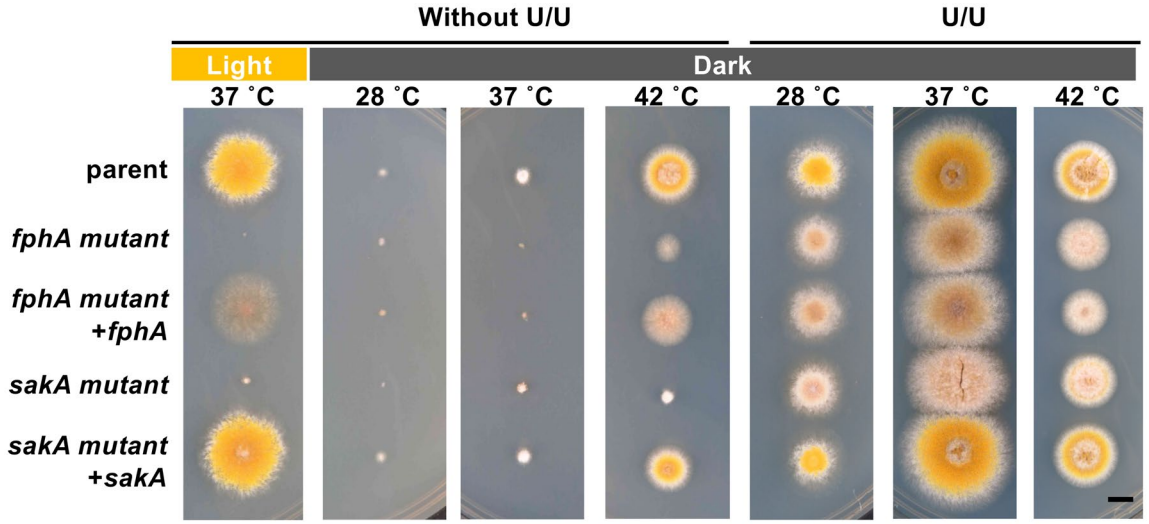

Fig. 2. Growth of different *A. nidulans* strains in light and at different temperatures. The strain used for mutagenesis (parent, SZY17) is characterized by light- or temperature-dependent growth in the absence of uracil and uridine (U/U). Growth of the *fphA* mutant (M10-13) and the *sakA* mutant (M6-9) is only partially restored at higher temperature. The strains were incubated 3 days under conditions as indicated. Scale bar, 0.5 cm.

formation was inhibited by light in wild type but less in the phytochrome-deletion strain. Sporulation of both wild-type and phytochrome-deletion strain was promoted. However, no phytochrome-dependent temperature effect on development was observed. At 42°C, all developmental processes were largely inhibited.

In order to obtain further evidence for a role of the phytochrome FphA in temperature sensing, the transcription of three genes was studied, *ccgA*, *ccgB* and *conJ* (Fig. 3 and Suppl. Fig. S2). Indeed, after temperature increase to 42°C, all three genes were significantly induced in wild type and the induction of transcription was drastically, but not completely, reduced in the *fphA* mutant. In the *sakA* mutant, the temperature effect on their transcription was completely lost. These results support the idea of a phytochrome thermosensor and another yet unknown thermosensor. Signal transduction of both apparently merges before or at SakA. Therefore, we tested the effect of double-deletion of *fphA* and *tcsB*. However, *ccgA* and *ccgB* were still responsive to heat stress to a similar extent in comparison to the *fphA*- or the *tcsB*-single mutants (Fig. 3).

Heat sensing leads to phosphorylation and nuclear shuttling of SakA

To test whether the temperature changes could cause the shuttling of the MAP kinase SakA into the nuclei, we compared the wild type (SZY34) with the *fphA*-deletion strain (SZY37). In both strains, SakA was tagged with GFP and expressed under its native promoter. At 28°C in the dark, SakA was evenly distributed in nuclei and the cytoplasm in both strains (Fig. 4A). Intriguingly, at 42°C, SakA shuttled from the cytoplasm into nuclei. Quantification of the GFP intensity in nuclei and the cytoplasm evenly in both strains revealed 2.5-fold accumulation in the nuclei in wild type and only 1.7-fold accumulation in the *fphA*-deletion strain (Fig. 4B). The shuttling of SakA in the absence of FphA indicates additional temperature-sensing mechanisms independent of phytochrome. The accumulation of SakA in the nucleus upon a temperature rise suggested SakA phosphorylation. A four-minute incubation at 42°C in the dark resulted indeed in increased phosphorylation of SakA. This increase was much stronger in wild type than in the *fphA* mutant (Fig. 4C and D). After eight minutes, the phosphorylation level of SakA decreased. This transient effect points to an autoregulation mechanism during temperature adaptation. The fact that transient phosphorylation increase was much stronger in wild type as compared to the *fphA* mutant strain supports the idea of phytochrome as thermosensor. All three experiments described above show also that phytochrome is not the only temperature sensor, because residual inductions by temperature are observed in the phytochrome loss-of-function mutants. These results show that phytochrome-dependent phosphorylation of SakA and nuclear import are involved in temperature sensing. However, phytochrome could additionally affect the transcription of *sakA* and/or other components of the HOG signaling pathway. Transcript analyses of *sskB*, *pbsB* and *sakA* revealed no evidence for such a link (Suppl. Fig. S4). Whether the described short-term changes of SakA activity are solely responsible for the observed long-term induction of the *conJ* promoter required for colony growth remains to be investigated.

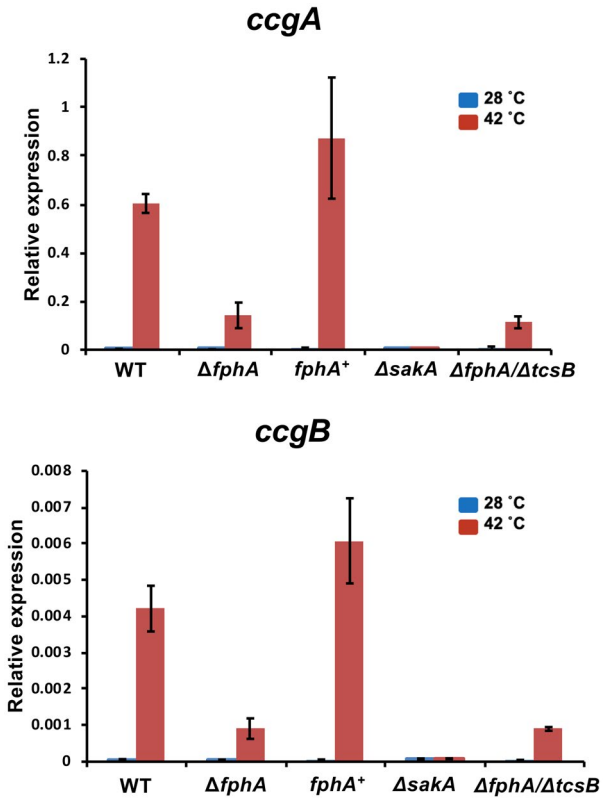

Fig. 3. Expression analysis of two light-responsive genes at different temperatures in wild type (WT), the Δ*fphA*, and the Δ*sakA* strains. Spores of WT (SJR2), the Δ*fphA*-strain (SJR10), the *fphA*-re-complemented strain (*fphA*$^+$, SJP22.1), the Δ*sakA*-strain (SZY31) and a Δ*fphA*/Δ*sakA*-double-deletion strain (SZY73) were cultured on the surface of supplemented minimal medium at 28°C for 18 h in the dark. The mycelia were then transferred onto the surface of fresh minimal medium, pre-warmed to 28 or 42°C and incubated for 10 min in the dark. Then, the mycelia were frozen immediately in liquid nitrogen followed by RNA isolation. The expression levels of *ccgA* and *ccgB* were normalized to the histone *h2b* gene. The bars present mean values ± SD of three biological replicates.

Temperature changes cause structural changes of phytochrome

If phytochrome serves as temperature sensor, one of its properties should change with temperature. UV/Vis absorption spectra might indicate protein conformational changes. Indeed, altered spectral properties at higher temperature have been described for bacterial phytochromes Agp1 and Cph1 (Kim *et al.*, 2014; Njimona *et al.*, 2014). Temperature-dependent dark reversion has been described for plant and bacterial phytochromes (Jung *et al.*, 2016; Legris *et al.*, 2016), and temperature sensing of plant phytochromes has been explained by effects on dark reversion. We therefore investigated the impact of temperature on the UV/Vis spectra of FphA in its Pr and Pfr forms and on dark reversion of FphA. The typical phytochrome core domain arrangement with the PAS/GAF/PHY tridomains and the histidine kinase domain is expanded in FphA by an N-terminal extension (NTE) and a C-terminal response regulator. In order to find possible impacts of different protein regions on temperature effects, we analyzed three FphA versions, full-length FphA, FphA without the N-terminal extension (FphAΔNTE) and the photosensory core module (PCM) which contains only the PAS GAF and PHY domains but lacks the N-terminal extension and the histidine kinase and response regulator domains (Fig. 5A). Absorbance spectra of the Pr and Pfr forms were measured in the range between 20 and 50°C (Fig. 5B–G). The Pr spectra of FphA were highly similar between 20 and 30°C. As in typical phytochrome spectra, the absorbance of the peak in the 700 nm range (Q-band) was high, whereas the peak in the 380 nm region (Soret band) had a lower absorbance. However, at higher temperature the absorbance of the Q-band decreased, whereas absorbance of the Soret band increased. The Q-band to Soret band ratio decreased continuously from 2.0 at 20°C to 0.43 at 50°C. The position of the Q-band maximum shifted from 705 to 690 nm. Free biliverdin measured in the same buffer solution at 20°C (Fig. 5B) had a Q-band to Soret band ratio of 0.33 and a Q-band maximum at 670 nm. Thus, the temperature increase changes Pr spectra of FphA toward the spectrum of free biliverdin (Fig. 5B). The chromophore of phytochromes is covalently attached to a cysteine and embedded in the chromophore pocket formed mainly by the GAF domain (Lamparter *et al.*, 2003; Blumenstein *et al.*, 2005). The typical spectral properties of phytochromes are determined by tight protein–chromophore interactions. We therefore assume that the similarity of the absorbance spectra with that of free biliverdin results from loosened chromophore–protein interactions or a 'softening' of the chromophore pocket due to an increase in structural dynamics. These altered properties correlate with activation of FphA in darkness.

The absorbance spectra also show that the protein does not form aggregates in the given temperature range, that is, there is no indication for denaturation. Photoconversion, another indicator for protein integrity, was possible up to 50°C, as indicated by difference spectra (Fig. 5H–J).

Similar temperature-induced spectral changes were observed for FphAΔNTE (Fig. 5C) and PCM (Fig. 5D). However, both fragments showed signs of protein aggregation at 50°C. The base absorbances of the respective curves increased with decreasing wavelengths, a clear sign for increased scattering due to increased particle size. Thus, in full-length FphA the NTE and the histidine kinase/ response regulator domains stabilize the protein against temperature denaturation.

Irradiating with red light results always in a mixture of Pr and Pfr. Characteristic absorbance spectra of red-irradiated phytochromes have either two peaks in the red

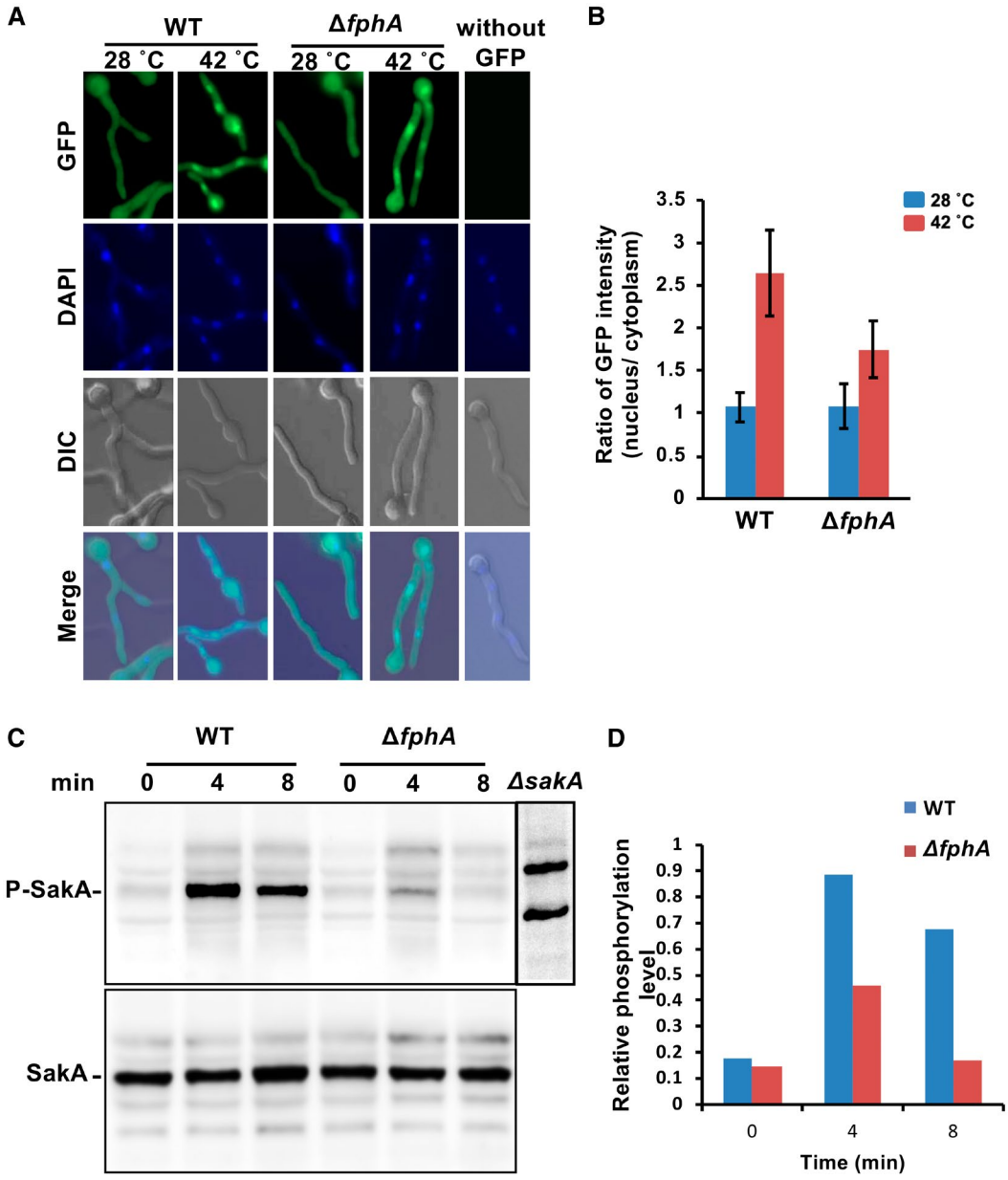

Fig. 4. Analysis of the MAP kinase SakA in response to temperature increase.
A. SakA-GFP shuttling into nuclei. Spores of wild-type (WT) (SZY34) and of the Δ*fphA* strain (SZY37) were inoculated on coverslips with 400 µl supplemented liquid minimal medium and incubated for 18 h at 28°C in the dark. Then, coverslips were dipped for three minutes into fresh medium pre-warmed at 28 or 42°C, and then, the samples were fixed with pre-warmed PBS containing 4% formaldehyde for 10 minutes before microscopy. Scale bar, 5 µm.
B. Quantification of SakA-GFP fluorescence in wild-type and the Δ*fphA*-strain. Microscopy settings were always identical. Of each strain, 30 cells were chosen to calculate the fluorescence ratios between nucleus and cytoplasm. Fluorescence intensities were quantified by the ZEN software (ZEISS); the bars present mean values ± SD.
C. SakA phosphorylation analysis. Each strain (SJR2 [WT], SJR10 [Δ*fphA*]) was cultured in the dark at 28°C in a 1 l flask with 400 ml supplemented minimal medium for 18 h and then 50 ml mycelial culture were transferred into flasks pre-warmed to 28 or 42°C and incubated for four or eight minutes. Mycelia were harvested and frozen immediately in liquid nitrogen for protein extraction. About 45 µg crude extract of each sample was loaded and analyzed in a Western blot using antibodies against phosphorylated SakA (P-SakA) or against SakA. The Δ*sakA* (SZY31) strain was used as a negative control for the phosphorylated SakA.
D. Quantification of the relative phosphorylation level of SakA in Fig. 3C.

and far-red spectral region or a peak and a shoulder. From these spectra together with Pr spectra, Pfr spectra and the relative fraction of Pfr (±5%) can be calculated in a semi-empirical way (Zienicke *et al.*, 2013). In FphA, the Pfr fractions decreased from 70% at 20°C to 30% at 50°C, and similar values were obtained for FpaAΔNTE and FphA-PCM. The calculated Pfr spectra of all three FphA versions show that a temperature increase results

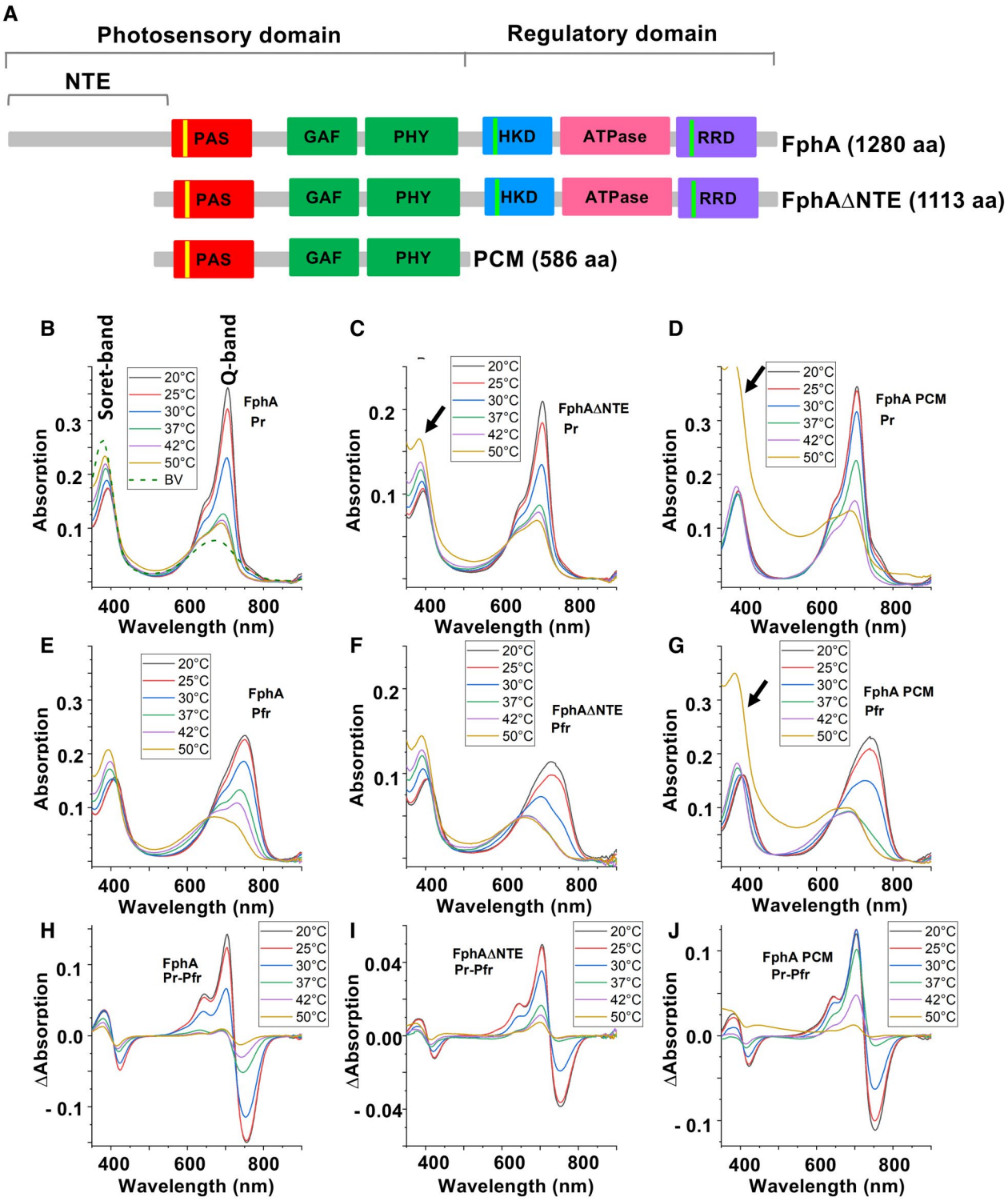

Fig. 5. Spectral properties of FphA variants at different temperatures.
A. Domain arrangement of the three FphA versions. FphA, full-length protein (1280 amino acid); FphAΔNTE, full-length protein without the N-terminal extension, NTE (1113 amino acid); PCM, photosensory chromophore module, C-terminal truncated version without NTE (586 amino acid). The domains and the crucial amino acid residues are indicated.
B–D. Absorption spectra of the Pr form of FphA (B), FphAΔNTE (C) and PCM (D) at different temperatures between 20 and 50°C as given in each panel. The samples were always kept in darkness or green safelight. In all constructs, temperature increase results in a decrease of the Q-band (around 700 nm) absorption and an increase of the Soret band absorption. The 50°C spectra of (B) and (C) are comparable with the spectrum of free biliverdin. The 50°C curve of (C) and (D) is characterized by wavelength dependent increase of basal absorption (arrows). This is a clear indication for increased scattering, resulting from protein aggregation.
E–G. Calculated Pfr spectra of FphA (E), FphAΔNTE (F) and PCM (G) at different temperatures as given in the panels. The dark-adapted proteins were irradiated for 2 minutes with red light and measured again. After such an irradiation, a mixture of Pr and Pfr is obtained. Based on these spectra and the Pr spectra, the presented Pfr spectra and the relative fraction of Pfr were calculated. The temperature-induced increase in scattering of FphA-PCM is also observed here (arrow in [G]).
In (H–J), difference spectra of FphA (H), FphAΔNTE (I) and PCM (J), at temperatures as given in the panels. For these, the Pfr spectra as given in (E–G) were subtracted from the Pr spectra as given in (B–D). These results show that the absorbance changes during photoconversion decrease with temperature increase and that light-induced spectral changes occur at all temperatures for all samples.

in a decrease of Pfr absorbance and a drastic shift of the Q-band maximum to shorter wavelengths (Fig. 5E–G). These temperature-induced spectral changes of Pr and Pfr will alter the photoequilibrium between these two states in continuous light in favor of Pr.

We also tested the effect of temperature on dark reversion of different FphA constructs. Pr spectra were first measured at 20°C, then at 37°C and after a temperature decrease of the same sample again at 20°C. In full-length FphA, the low Q-band absorbance that was obtained at 37°C remained low after back-shift to 20°C (Fig. 6A). In other words, the temperature-induced softening of the chromophore pocket remained upon subsequent cooling, that is, is irreversible. On the contrary, the Q-band absorbance of FphAΔNTE (Fig. 6B) and of PCM (Fig. 6C) recovered partially and almost completely during the temperature decrease respectively. Thus, the NTE and the histidine kinase/ response regulator domains together keep the chromophore pocket in a softened state.

We also tested for a temperature effect on Pfr-to-Pr dark reversion. As in previous measurements (Brandt *et al*., 2008), dark reversion of FphA at 20°C was very slow (Fig. 7A). During 1 h, only ca. 2.5 % Pfr converted back to Pr, that is, under these conditions the effect of dark reversion on Pfr levels in light is negligible. We observed an increase in the rate of dark reversion at higher temperature (Fig. 7A). During 1 h, ca. 30% of Pfr reverted back to Pr. In light, the spectral overlap of Pr and Pfr and the increased dark reversion at elevated temperature will result in a lower relative Pfr proportion as compared to moderate temperature.

Dark reversion and the temperature effect on it were significantly dependent on the domain composition. Both truncated proteins had a faster dark reversion at 20°C (Fig. 7B and C) than full-length FphA (Fig. 7A). However, the kinetics of the dark reversion of the PCM protein looked very different with a strong increase in the first minutes until a plateau was reached. This could indicate that only a fraction of the proteins was able to undergo dark reversion. In the case of the PCM protein, the temperature increase to 42°C accelerated dark reversion, as in full-length, whereas FphAΔNTE exhibited slower dark reversion than the other two proteins at elevated temperature (Fig. 7B). Thus, the presence of the NTE inhibits dark reversion and is required for the pronounced temperature effect on dark reversion. The role of the histidine kinase/ response regulator domains is less clear (Fig. 7C).

Altogether, we see here a remarkable difference between fungal FphA and plant phytochrome B with respect to combined light and temperature effects. In plant phytochrome B, the Pfr level under illuminating conditions is dependent on temperature *via* dark reversion (Jung *et al*., 2016; Legris *et al*., 2016), whereas in fungal FphA, temperature-dependent Pfr levels (Fig. 7D) are largely determined by spectral changes of the chromophore. Activation of the fungal phytochrome can be triggered by light or independent of light by temperature.

Temperature sensing in A. alternata

In order to see if the role of phytochrome in thermosensing is conserved in other fungi, we analyzed phytochrome of *A. alternata*. Therefore, we expressed the photosensory domain of Alternaria FphA in *Escherichia coli* and analyzed it spectroscopically at different temperatures as before the Aspergillus FphA (Suppl. Fig. S6A and B). Upon shifting from 15 to 50°C, which is the highest temperature Alternaria FphA can withstand, we observed a 10% decrease of the absorption of the Pr form. After shifting the sample back to 15°C, the spectrum fully recovered. Scattering occurred only in samples, which were shifted to 60°C, which indicates denaturation and aggregation of the protein.

The last question was whether the observed function of phytochrome had similar effects on gene transcription as in *A. nidulans* and any impact on *A. alternata in vivo*. Indeed, the transcripts of the *ccgA* gene and the catalase genes (*catA*, *catB* and *catD*) were upregulated

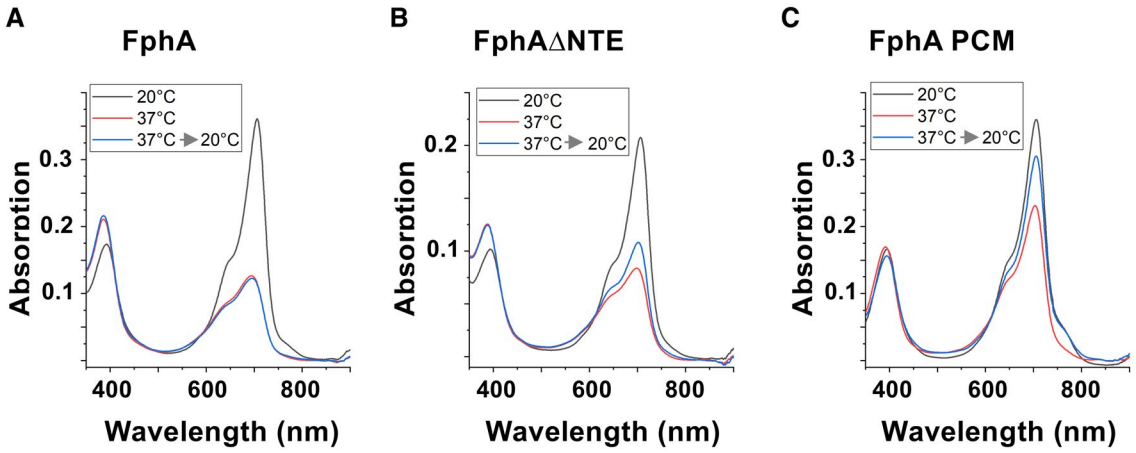

Fig. 6. Spectral properties of the Pr form of FphA variants during lowering and rising the temperature. Absorption spectra of (A) FphA, (B) FphAΔNTE and (C) PCM were first measured at 20°C (black lines); then, the samples were heated to 37°C and measured again (red lines) and finally cooled down to 20°C and measured for a third time (blue lines).

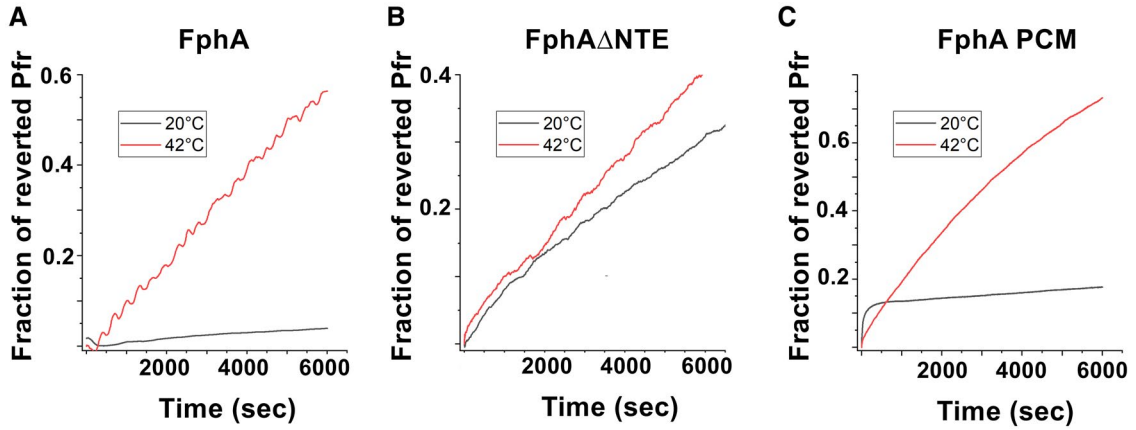

Fig. 7. Dark reversion of FphA variants at 20 and 42°C monitored at 705 nm. The 705 nm absorbance of (A) FphA, (B) FphAΔNTE and (C) PCM was continuously recorded in the dark after saturating red irradiation. Measurings were performed at 20 and 42°C. An absorbance increase indicates an increase of P_r. Both curves are normalized to $A_{705\ nm}$ at $t_0 \triangleq 0$ and $A_{705\ nm}$ of Pr $\triangleq$ 1. Representative measurements from 3 or more repetitions are shown.

upon temperature shift from 28 to 33°C in WT in the dark but not in the *fphA*-deletion strain. *catD* was even down regulated (Fig. 8A). Sporulation and radial growth of the *fphA*-deletion strain were more sensitive to a temperature shift in comparison to the WT strain. Temperature shift did not affect conidia formation of the WT strain in the dark. In the *fphA*-deletion strain, less conidia were produced at 33°C than at 28°C (Fig. 8B and C). Additionally, the effect of red light on promoting sporulation at 28°C was nullified after a temperature shift to 33°C in WT. The lack of FphA resulted in reduced radial growth at 33°C compared to WT (Fig. 8D and E).

Discussion

We describe here a role of two hybrid histidine kinases, TcsB and the phytochrome FphA in temperature sensing in *A. nidulans* and of phytochrome in *A. alternata*. We found that temperature increases activate the HOG signaling MAP kinase pathway in a similar way as light does (Yu *et al.*, 2016; Yu and Fischer, 2019) and cause the activation of several genes (Fig. 9). This raises the question about the molecular function of FphA in the temperature response. Phytochrome has at least two functions in the cell, one in the cytoplasm and one in the nucleus (Blumenstein *et al.*, 2005; Purschwitz *et al.*, 2008; Purschwitz *et al.*, 2009). There is evidence that phytochrome interacts in the nucleus with other regulators involved in light signaling, such as VeA, and also with proteins involved in chromatin remodeling, such as GcnE (Purschwitz *et al.*, 2008; Hedtke *et al.*, 2015). Temperature activation of FphA could change that interaction network and cause the observed changes in gene expression. This possibility has not been tested yet. In

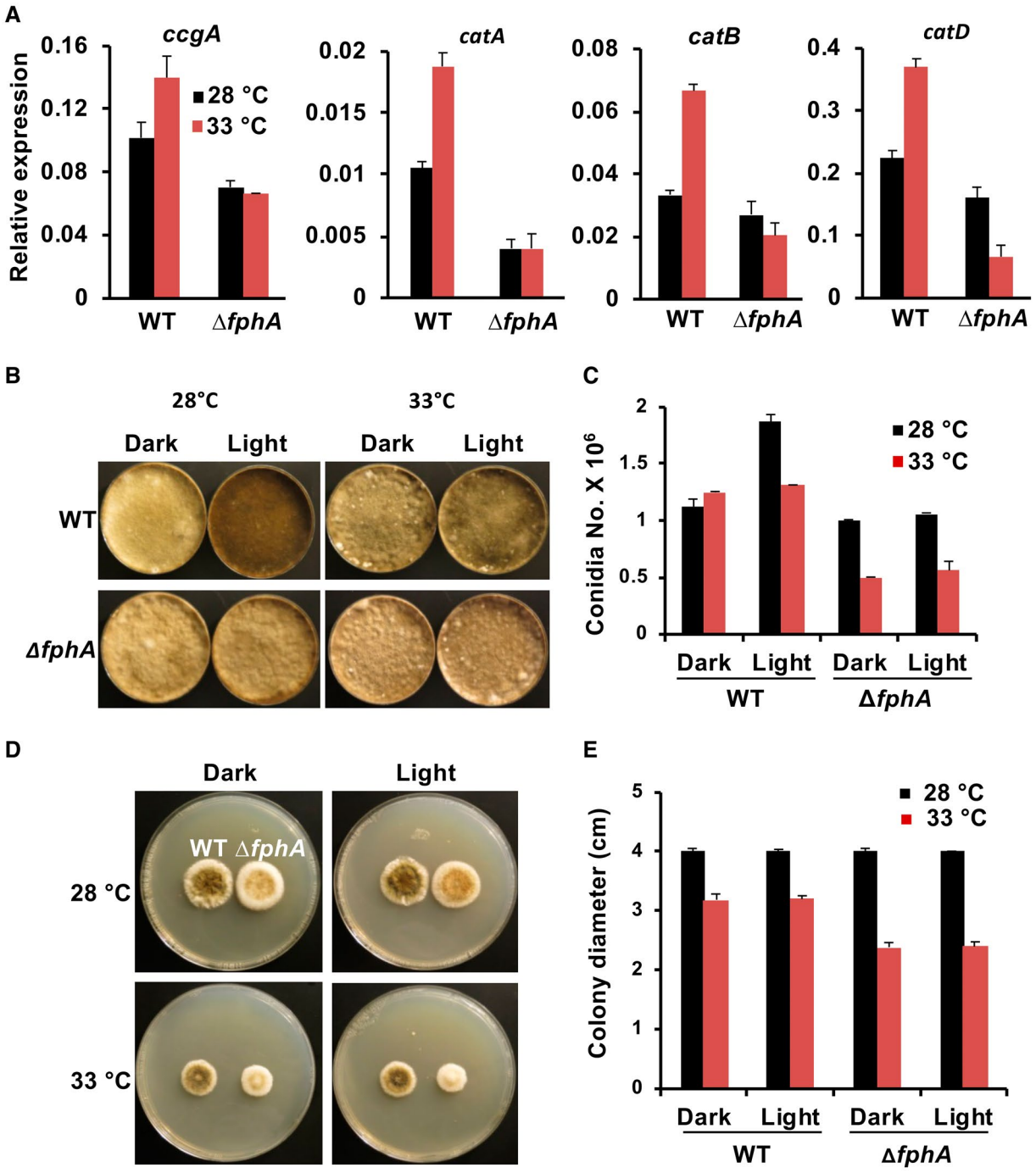

Fig. 8. Temperature sensing in *A. alternata*.
A. Expression analysis of light-responsive genes at different temperatures in *A. alternata* wild-type (WT, ATC66981) and the Δ*fphA* strain (SOI1). Spores of WT and SOI1 were cultured on the surface of mCDB at 28°C for 40 h in the dark. The mycelia were then transferred onto the surface of fresh mCDB pre-warmed to 28 or 33°C and incubated for 15 minutes in the dark. Then, the mycelia were frozen immediately in liquid nitrogen followed by RNA isolation. The expression levels of *ccgA*, *catA*, *catB* and *catD* were normalized to the histone *h2b* gene. The bars present mean values ± SD of three biological replicates.
B. Colony appearance on mCDB plates inoculated with 5000 conidia evenly spread on the agar surface and incubated at 28 and 33°C for 12 days in the dark or under red light (700 nm, LEDs).
C. Quantification of the conidia produced on the plates in panel (B). Three independent plates of each strain were analyzed, and the mean values for the three samples are displayed. The arrow bar represents the standard deviation.
D. Pictures of colonies of the WT and the *fphA* mutant strain incubated at 28 and 33°C for 5 days.
E. Colony diameters from the colonies in (D). The experiments were repeated three times, and the arrow bar represents the standard deviation.

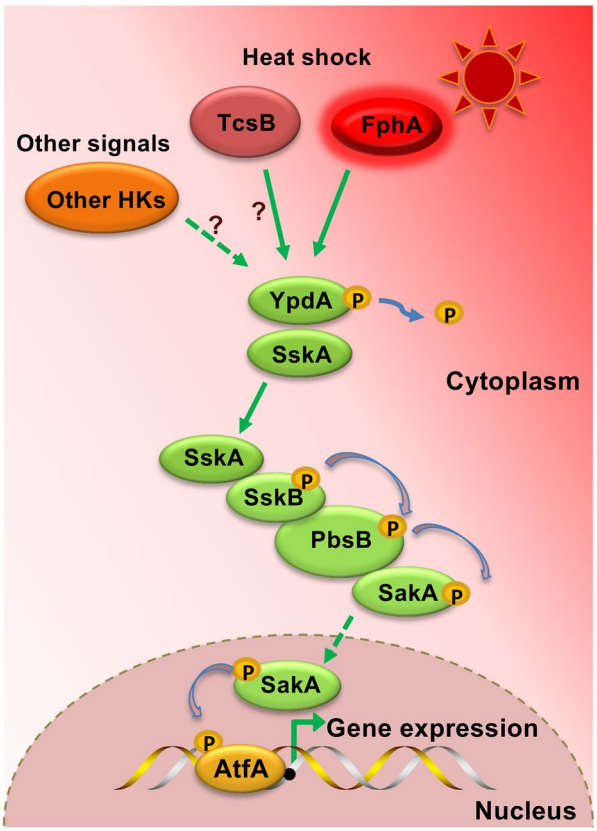

Fig. 9. Scheme of light and temperature sensing in *A. nidulans.* Light causes phytochrome-dependent activation of the signaling cascade. The primary event is the control of the phosphorylation status of YpdA. The second hybrid histidine kinase, TcsB, may also interact with YpdA, although this has not been shown yet. Other hybrid histidine kinases may account for the residual head activation of the reporter genes in the absence of *fphA* and *tcsB*.

the cytoplasm, FphA interacts with the phosphotransfer protein YpdA and thereby activates the HOG pathway (Yu *et al.*, 2016). In both cases, it is conceivable that phytochrome acts as a sensory protein and hence as a molecular 'thermometer'. This view is supported by our spectral analyses, which we interpret in such a way that the chromophore-binding pocket is softened. This shows that temperature changes cause structural changes of the phytochrome protein which lead to the downstream effects. This view is well supported by recent work with plant phytochrome (Casal and Qüesta, 2018; Park and Park, 2019).

In the following, we are going to discuss several of our findings in more detail. The spectral analyses of FphA *in vitro* revealed several temperature effects. Two mechanisms are expected to result in lowering the relative Pfr content in light at increasing temperature, dark reversion and changes of the extinction coefficient causing the decrease of the Q-band. Temperature has thus a similar effect on Pfr levels as in plant phytochromes. These temperature effects are, however, less relevant in *A. nidulans* because FphA responds to temperature also in darkness. Quite remarkably, the temperature effects were observed in darkness, opposed to the temperature effects that have been described for *Arabidopsis* that required light (Jung *et al.*, 2016; Legris *et al.*, 2016; Rockwell and Lagarias, 2017).

With the recombinant fungal phytochrome FphA, it was possible to find significant temperature effects on the absorbance spectra. For both Pr and Pfr spectral forms of FphA, the Q-band absorbance decreased and the Soret band absorbance increased with increasing temperature for all three protein versions of FphA. Denaturation and aggregation at 50°C was only obtained for *A. nidulans* FphA without the N-terminal extension (FphA-ΔNTE) or only the photosensory domain (PCM). In *A. alternata,* inactivation of the protein started at 60°C. Our conclusion from these observations is that the interplay between histidine kinase/ response regulator domain, PCM and NTE together stabilizes the entire protein at elevated temperatures. FphA seems to be optimized for higher temperatures. We assume that the spectral changes correlate with the induction of temperature effects either originating from the PCM via interacting partners or via intramolecular signal transduction to the histidine kinase or NTE and then to other partners. One candidate for the interaction with FphA is the phosphotransfer protein YpdA, where a direct interaction was shown (Yu *et al.*, 2016). However, there is evidence that phytochrome is also involved in chromatin remodeling and may interact with the histone-modifying enzyme GcnE (Hedtke *et al.*, 2015).

We interpret the spectral changes of FphA with rising temperatures, leading to spectra which resemble the free chromophore, as resulting from a 'softening' of the chromophore pocket. Similarly, temperature dependence of UV/Vis spectra of the BLUF protein BlsA from *Acinetobacter baumannii* was attributed to a loss of rigidity of the FAD-binding pocket with increasing temperatures (Abatedaga *et al.*, 2017). The temperature-induced changes of spectral properties were not reversible for full-length FphA. Data of the truncated fragments, which reveal partial reversion of spectral properties upon warming and cooling, suggest that both the NTE and the histidine kinase/ response regulator domains are required for the memory effect (Fig. 5B–D). The histidine kinase generally functions as dimerization site, and the memory effect could be based on dimer formation by histidine kinase and NTE in which the chromophore pocket in the softened state is stabilized by interaction with the respective other subunit. However, size-exclusion chromatography suggested that all three variants are dimeric or oligomeric (data not shown). We therefore propose that the memory effect is mediated through a direct impact of the NTE and the

histidine kinase/ response regulator domains on the PCM. Since the temperature in *A. nidulans* is sensed also in darkness, dark reversion of FphA is not required for temperature sensing. If both Pr and Pfr are equally active with respect to induction of stress responses, it would not matter whether or not there is dark reversion at these temperatures. An increase of dark reversion with the temperature could simply result from activation barrier overcome. That the temperature effect on dark reversion is less pronounced in FphA without NTE shows, however, that the NTE has especially evolved to modulate dark reversion at higher temperature.

Despite large phylogenetic distances between plants, bacteria and fungi, a previously unexpected thermometer function has been described for all three groups. Does this mean that such a function is intrinsic and evolutionarily conserved or has this second function of phytochrome been evolved independently in each group? The thermosensing activity in darkness found here for a fungal phytochrome contrasts with the corresponding described phytochrome action in plants which is based on dark reversion and might occur only in light. This difference points to different mechanisms behind phytochrome-based thermometers. In plants, a dogma predicts that Pr has no physiological activity because phytochrome mutants or plants overexpressing phytochrome have always a wild type like phenotype in darkness (Boylan and Quail, 1991; Wagner *et al.*, 1991). Therefore, an effect of Pr at elevated temperature was not tested. In another study, differences between the *Arabidopsis phyB* mutant and wild type at 37°C have however been reported (Njimona *et al.*, 2014). Also, the inhibition of conjugation in *A. fabrum* at higher temperature was observed in darkness (Bai *et al.*, 2016). The histidine kinases of many bacterial phytochromes are more active in the Pr form. One can therefore imagine that phytochromes act as thermometers in general in both Pr and Pfr forms and that light and temperature signals are integrated on the level of these chromoproteins. Above ground, temperature and sunlight are closely coupled in nature. Underground where light is weak, temperature still provides information, for example, about the day–night cycle. Likewise, both temperature and light synchronize circadian clocks, present in many organisms (Dunlap and Loros, 2017). Given that there is some biochemical evidence that the phytochrome from the aquatic (marine and freshwater) cyanobacterium Synechocystis PCC6803, Cph1, also acts as temperature sensor (Njimona *et al.*, 2014), we are tempted to speculate that temperature sensing could be the ancient function of phytochromes that was already present before the photoreceptor function of this family of proteins evolved. There is evidence that blue-light receptors such as phototropin or BLUF photoreceptors also respond to temperature (Abatedaga *et al.*, 2017; Fujii *et al.*, 2017).

Temperature-induced phenotypic changes were only partially dependent on phytochrome in the case of *A. alternata* or apparently independent as in the case of *A. nidulans*. This apparent contradiction is probably due to the different time scales. Whereas the effect on gene transcription occurs in minutes, effects on colony growth or sporulation take one to several days. Our results suggest that phytochrome is especially required for fast responses to the ambient temperature. However, we also have to consider that the conditions on agar plates under laboratory conditions are very different from the growth conditions in nature. It is well conceivable that under natural conditions, phytochrome plays a much more prominent role. In addition, it is clear that TcsB plays some role in temperature sensing (Fig. 9) and perhaps some other proteins as well. The biological response to temperature changes therefore appears to be rather complex.

Given that temperature changes play a crucial role in some fungi to adapt to different niches, it will be most interesting to see if mutation of phytochrome, for example, influences the dimorphic switch in the pathogenic *P. marneffei* or whether it has an impact on the pathogenic growth of *A. fumigatus* (Boyce and Andrianopoulos, 2015; van de Veerdonk *et al.*, 2017).

Experimental procedures

Strains, plasmids and culture conditions

Supplemented minimal medium (MM) for *A. nidulans* was prepared as described, and standard strain construction procedures were used (Käfer, 1977). *A. alternata* cultures were grown on modified Czapek–Dox broth (mCDB) agar if not stated differentially and incubated 1 to 12 days at 28°C. Strains used in this study are listed in Table 1. To construct the *ΔshoA* (SZY70), *ΔtcsB* (SZY72) and *ΔfphA/ΔtcsB* (SZY73) mutants, the nutritional marker gene *pyrG* deriving from *A. fumigatus* was fused with the left and right boarders of the *shoA* and the *tcsB* genes respectively. The fused cassettes were transformed into the SJR2 (wild type) or SJR10 (*ΔfphA*) strains to replace the *shoA* or *tcsB* genes by homologous recombination. Positive transformants were confirmed by Southern blotting or PCR.

Strain BL21 (DE3) was used for heterologous expression. Synthetic FphA, codon-optimized for *E. coli*, was cloned in the pASK-IBA3 vector (Brandt *et al.*, 2008). For the construction of an expression plasmid containing full-length FphA without the N-terminal extension (NTE) (1113 amino acid, FphAΔNTE) or the photosensory domain without NTE (586 amino acid, PCM), the polymerase chain reaction was performed according to manufacturer protocols with Q5 polymerase and using the plasmid pASK-*fphA*_syn as template. Primers used in this study were listed in Table 2. The *A. alternata* FphA photosensory domain (PCM, 587 amino acid) was cloned using the NEB NEBuilder® HiFi DNA Assembly Cloning Kit.

Table 1. Strains used in this study.

Strain	Genotype	Reference
A. nidulans		
SKV103	*pyrG89; pyroA4; veA+*	Vienken and Fischer (2006)
SJR2	*pyrG89; pyroA4; nkuA::bar; veA+*	Herr and Fischer (2014)
SRJ8	*pyroA4; nku::bar; veA*$^{+}$	Julian Röhrig, Karlsruhe
SJP1	*pyrG89; ΔargB::trpCΔB; pyroA4; ΔfphA::argB; veA+*	Purschwitz *et al.* (2008)
SJP22.1	SJP1 transformed with pJP19 (*fphA* with native promoter, *pyr4*)	Purschwitz *et al.* (2008)
SJP70	*pyrG89; ΔlreB::argB; ΔargB::trpCDB; pyroA4; veA*$^{+}$	Purschwitz *et al.* (2008)
SJR10	*pyrG89; ΔargB::trpCΔB; pyroA4, nkuA::bar; ΔfphA::argB; veA*$^{+}$	Hedtke *et al.* (2015)
SZY17	SKV104 transformed with pZY19 (*conJ(p)::pyr4, pyroA*)	Yu *et al.* (2016)
SZY18.2	*blind* mutant M6-9, *sakA* mutant	Yu *et al.* (2016)
SZY29	M10-13 re-complemented with *fphA* gene	Yu *et al.* (2016)
SZY23	*blind* mutant M10-13, *fphA* mutant	Yu *et al.* (2016)
SZY31	*pyrG89; ΔsakA::AfriboB; pyroA4, ΔnkuA::argB; veA*$^{+}$	Yu *et al.* (2016)
SZY34	*pyrG89; sakA(p)::sakA::GFP::AfpyrG; pyroA4, nkuA::bar; VeA*$^{+}$	Yu *et al.* (2016)
SZY37	*ΔargB::trpCΔB, sakA(p)::sakA::GFP::AfpyrG; pyroA4, nkuA::bar; ΔfphA::argB; veA*$^{+}$	Yu *et al.* (2016)
SZY45	M6-9 complemented with the *sakA* gene	Yu *et al.* (2016)
SZY70	*pyrG89; ΔshoA::AfpyrG, pyroA4; nkuA::bar; veA+*	This study
SZY71	SZY70 co-transformed with the *shoA* and the *AfpyroA* genes	This study
SZY72	*pyrG89; pyroA4,nkuA::bar; ΔtcsB::AfpyrG; veA*$^{+}$	This study
SZY73	*pyrG89; ΔargB::trpCΔB; pyroA4, nkuA::bar; ΔfphA::argB, ΔtcsB::AfpyrG; veA*$^{+}$	This study
A. alternata		
ATCC 66981	*A. alternata* wild type	Christopher Lawrence (Blacksburg, VA)
SOI1	*fphA* mutant Δ*fphA528* 528 nucleotides deleted by CRISPR cas 9 directed side mutagenesis	This study
E. coli		
Top10	F- *mcrA* cr *mrr-hsd*RMS-*mcr*BC) Φ 0*lac*Zac hsd *lac*X74 *rec*A1 *ara*D139 sd *araleu*)7697 *gal*U *gal*K *rps*L (StrR) *end*A1 *nup*G	Invitrogen, Leek, NL
BL21	F^{-} *ompT hsdS*$_B$ (r$_B^-$ m$_B^-$) *gal dcm* (DE3)	Novagen, Darmstadt

Analysis of asexual spores and cleistothecia under different conditions

To compare the phenotype of wild-type and *ΔfphA* strains, fresh conidia were inoculated in minimal medium with 0.75% agar at a spore density of 7.5×10^4 cells ml^{-1} before the medium solidified. About 1 ml medium with conidia was distributed evenly on each minimal medium plate (Ø 5.5 cm). The solidified plate was overlaid with 4 ml liquid medium and incubated at 37°C in the dark for 20 h. Then, the liquid medium was carefully discarded. The plates were incubated at different temperatures in darkness or in light (white light) for 24 h to quantify the number of conidia or 5 days for the quantification of cleistothecia.

Fresh conidia of *A. alternata* wild-type and *ΔfphA* strains were grown on modified Czapek Dox broth (mCDB) agar and incubated 1 to 12 days at 28 and 33°C, respectively, under red light (680 nm) and dark conditions. Conidia were harvested in sterile tween 20, filtered for separation from mycelium and concentrated by centrifugation. The number was counted in a Neubauer counting chamber.

RNA isolation from A. nidulans *and reverse transcription quantitative PCR (RT-qPCR)*

Fresh conidia were inoculated on the surface of liquid supplemented minimal medium in Ø 3.5 cm petri dishes and cultivated in the dark for 18 h. The mycelia were transferred onto the surface of pre-warmed medium at 28 and 42°C, respectively, and incubated for 8 minutes. The mycelia were harvested in dim-green light and frozen immediately in liquid nitrogen. A 'Fungal RNA Extraction Kit' from Omega was used to isolate RNA, and cell disruption was performed with a cell homogenizer at 30 hits min^{-1} for 5 minutes. RNA was treated with TURBO DNA-free kit and diluted to 50 ng μl^{-1} with DEPC water. RT-qPCR was performed with SensiFAST SYBR & Fluorescein One-Step Kit from Bioline (Luckenwalde, Germany). Each reaction was carried out using 25 μl with 0.2 μM primers and 100 ng RNA. The program started with 10 minutes of the reverse transcription reaction at 45°C, followed by 2.5 minutes at 95°C for the inactivation of the reverse transcriptase and 40 cycles of polymerase chain reaction (10 s at 95°C and then 30 s at 58°C). To assess the dissociation characteristics of two-stranded DNA, melting curve analyses were carried out (80 cycles, 95 to 58°C with 10 s per step). The *h2b* gene was used for normalization. Each transcript level is the average of three biological replicates.

A. alternata conidia were inoculated with a loop on the surface of 20 ~ 25 ml of complete liquid medium mCDB in a petri dish. After 40 h of incubation in darkness at 28°C, the mycelia were transferred onto the surface of a pre-warmed medium at 28 and 33°C, respectively, and incubated for 15 minutes. The mycelia were collected and stored as described above until further analysis. RNA was isolated with the same kit as above, and RT-qPCR was performed with the same procedures.

Table 2. Oligonucleotides used in this study.

Name	Sequence (from 5′ to 3′)	Description
ShoA_L_F	CCTCGTTCTTCTTACCTCAC	Fusion PCR for amplification of the *shoA* ORF knockout cassette
ShoA_L_R	ATCCACTTAACGTTACTGAAATCGTTGAGTCGATCTGCTGTAG	
ShoA_R_F	CTCCTTCAATATCATCTTCTGTCGACTTCAGCCTCTCGTATG	
ShoA_R_R	GTCCAGCCCAGTAATAGAAG-3'), pyrG_F (5'-GATTTCAGTAACGTTAAGTGGAT	
pyrG_F	GATTTCAGTAACGTTAAGTGGATCAA	
pyrG_R	GACAGAAGATGATATTGAAGGAG	
TcsB_LB_F	GTTCTTGCTGAGTCTTCTGACATTGC	Fusion PCR for amplification of the *TcsB* ORF knockout cassette
TcsB_nest_F	CGGCCTCACTTGAGTTATGATCGT	
TcsB_LB_R	CCCGTTCATATCCAGCGAGGAT	
TcsBpyrG_F	ATCCTCGCTGGATATGAACGGGGATTTCAGTAACGTTAAGTGGATCA	
TcsBpyrG_R	GCATGGTTTGCTAGGCTCCCGACAGAAGATGATATTGAAGGAGCC	
TcsB_RB_F	GGGAGCCTAGCAAACCATGC	
TcsB_nest_R	TCCAGCTCGACAAGTATCTGATCG	
TcsB_RB_R	CCAACACACTAAAGGGTCCCTAGAC	
FphAΔNTE_XbaI_F	CCCTCTAGAAATAATTTTGTTTAACTTTAAGAAGGAGATATACATATGACCACC CGTTTTCGTCATG	Heterologous expression of FphA mutatants in *E. coli*
FphAΔNTE_NcoI_R	CGCCATGGTCGCTATGGGTATACGGGGTAAACC	
FphA-PCM_XbaI_F	CCCTCTAGAAATAATTTTGTTTAACTTTAAGAAGGAGATATACATATGACCAC CCGTTTTCGTCATG	
FphA-PCM_NcoI_R	CGACCATGGGCCGCTTCCTGCTGACGC	
pASK_Alternaria_PCM_F	GAAATGAATAGTTCGACAAAAATCTAGAAATAATTTTGTTTAACTTTAAGAAGGA GATATACATATGTTTAAGCATGTCACTAC	
pASK_Alternaria_PCM_R	TGCGGGTGGCTCCAAGCGCTGAGACCATGGGCTGCTTCCTTCTGG	
h2b-RT-F	CTGCCGAGAAGAAGCCTAGCAC	RT-qPCR primers for *A. nidulans*
h2b-RT-R	GAAGAGTAGGTCTCCTTCCTGGTC	
ccgA-RT-F	CGACGCTTCCCTCACTTCTC	
ccgA-RT-R	CATCATGGGACTTCTCGTCCTT	
ccgB-RT-F	GGAGACTATCAAGGTAAGCATGTACC	
ccgB-RT-R	CTTGTCAAAGAGAGCGTCCTTG	
AlccgA-RT-F	GTCAACTCTGTCAAGAACGC	RT-qPCR primers for *A. alternata*
AlccgA-RT-R	TTGATCTTGTCACCAGCAGC	
AlcatA-RT-fw	GGCATTCTTACCGACACATCG	
AlcatA-RT-R	TGTGTAGAACTTGACGGCGAAA	
AlcatB-RT-F	CCACGGCACCTTTGTTTCTT	
AlcatB-RT-R	AGATCGGTGTCTCCTTTCCT	
AlcatD-RT-F	CAACGTCTCCCTCGACAAG	
AlcatD-RT-R	CAGTGAGAAGCATCAAGTCGG	
Alh2b-RT-F	ACAAGAAGAAGCGCACCAAG	
Alh2b-RT-R	CGTTGACGAAAGAGTTGAGAA	

Protein extraction from A. nidulans *and immunoblot detection*

Each *A. nidulans* strain was cultured in a 1 l flask with 400 ml supplemented minimal medium for 18 h at 28°C in the dark. Then, 50 ml culture was transferred into 250 ml flasks which were pre-warmed at 28 or 42°C in a water bath and incubated for 4 or 8 minutes. The mycelia were harvested immediately and frozen in liquid nitrogen for protein extraction under dim-green light. Mycelia were ground in a mortar with liquid nitrogen and afterward the mycelial powder collected into Eppendorf tubes. About 0.8 ml protein extraction buffer (20 mM Tris HCl, pH 8, 0.05% Triton X-100, 150 mM NaCl) containing phosphorylase inhibitor, protease inhibitor cocktail and 1 mM PMSF was added into each Eppendorf tube and incubated on ice for 20 minutes. The samples were centrifuged twice at 13,000 rpm and 4°C. After each centrifugation step, the supernatants were moved to new Eppendorf tubes and the pellets were discarded. The protein concentrations (quantified with the Bradford protein assay) were adjusted to the same final concentrations using protein extraction buffer. After denaturing, samples were loaded onto a 10% sodium dodecyl sulfate–polyacrylamide gel and blotted to a nitrocellulose membrane. For immunodetection, anti-phospho-p38 MAP kinase (The180/Tyr182) antibodies (Cell Signaling Technology; Beverly, MA; dilution 1:1000) against phosphorylated SakA/HogA, anti-Hog1p C-terminus antibody (Santa Cruz Biotechnology; California, USA; dilution 1:500) against SakA/HogA and anti-rabbit IgG (whole molecular)-peroxidase antibody (A0545; Sigma-Aldrich; München, Germany; dilution 1:80,000) were used.

Microscopy

To determine SakA localization in the wild-type and the *fphA*-deletion strain, fresh conidia were inoculated on coverslips with supplemented minimal medium and incubated 18 h in the dark at 28°C. Samples were then dipped into prewarmed fresh medium at 28 or 42°C for 3 minutes. Then, samples were fixed with PBS containing 4% formaldehyde for 10 minutes and washed once with PBS before observation. Fluorescence microscopy was performed with the

AxioImager Z1 (Zeiss), with the software AxioVision V4.5 and Zen with the AxioCam MR. A 63× Plan-ApoChromat objective was used. The light source was Osram HBO100.

Recombinant expression in E. coli *and purification of FphA variants*

To obtain phytochrome variants with the assembled biliverdin chromophore, FphA plasmids (pASK-IBA3_FphAsyn, pASK-IBA3_FphAΔNTEsyn and pASK-IBA3_PCMsyn plasmids) were expressed in *E. coli* BL21 (DE3) harboring the hemeoxygenase BphO from *P. aeruginosa* encoded in plasmid BphO_pACYCDuet (Brand *et al*., 2008). To obtain holo-PCM from *A. alternata*, *E. coli* BL21 (DE3) cells were contransformed with the plasmid encoding PCM and the plasmid pAT-BV harbouring the ho1-coding region from *Synechocystis sp. PCC6803* without the *pcyA*-coding region (Brand *et al*., 2008). The strains were grown at 37°C in 0.5 L LB medium containing 50 μg ml^{-1} ampicillin and 30 μg ml^{-1} chloramphenicol to an OD_{600} of 0.8–1. Bilin biosynthesis was induced by adding 500 μM IPTG 1 h before the induction of FphA. FphA or its variants were induced by the addition of 0.2 μg ml^{-1} anhydrotetracycline, and cells were incubated overnight at 20°C. The bacterial pellet of a 1 l culture was suspended in 10 ml extraction buffer (50 mM Tris HCl pH 7.8, 300 mM NaCl, 10% glycerol, 0.05% Tween 20, 5 mM DTT, 1 mM PMSF). Cells were lysed using a French Press at a pressure of 1000 bar, and the cell debris was removed by centrifugation. The supernatant was incubated with 40 μM ml^{-1} avidin for 15 minutes on ice and loaded onto a 2 ml *StrepTactin–Sepharose* column (IBA). Subsequent purification steps were performed according to the manufacturer's instructions. All steps were performed under a green safelight or in the dark.

Absorption spectra and dark reversion at various temperatures

Spectra were recorded in a JASCO V-550 photometer with a temperature control unit and a custom-built computer-controlled irradiation device. For measurements of the Pr spectra, the sample was always kept in darkness or green safelight. The temperature adjustment by the temperature control unit was controlled by measurements inside the cuvette. To obtain spectra of photoconverted FphA, the purified protein was irradiated for 2 minutes with red light from light-emitting diode (655 nm, 370 μmol $m^{-2}s^{-1}$) prior to spectral scan. For back conversion into the Pr form, the sample was irradiated for 2 minutes with far-red light (780 nm, 3000 μmol $m^{-2}s^{-1}$). For temperature reversion measurements, the absorption spectra of the FphA variants were measured at 37°C, and then temperature was brought back to 20°C and the spectra measured again. The samples were irradiated with far-red light for 2 min before each measurement. For dark reversion measurements, the samples were initially irradiated with red light for 2 minutes; then, the light was switched off and the absorption at 705 nm was continuously recorded. The data were scaled between the lowest possible (≙ 0, after red irradiation) and the highest possible (≙ 1, as in dark-adapted stage) 705 nm absorbance values.

Acknowledgement

This work was supported by the German Science Foundation (DFG, Fi459/19-1). Z.Y. was a fellow of the CSC. We thank Birgit Schreckenberger for excellent technical assistance.

References

Abatedaga, I., Valle, L., Golic, A.E., Muller, G.L., Cabruja, M., Moran Vieyra, F.E., *et al*. (2017) Integration of temperature and blue-light sensing in *Acinetobacter baumannii* through the BlsA sensor. *Photochemistry and Photobiology*, **93**, 805–814.

Bai, Y., Rottwinkel, G., Feng, J., Liu, Y. and Lamparter, T. (2016) Bacteriophytochromes control conjugation in *Agrobacterium fabrum*. *Journal of Photochemistry and Photobiology B: Biology*, **161**, 192–199.

Blumenstein, A., Vienken, K., Tasler, R., Purschwitz, J., Veith, D., Frankenberg-Dinkel, N. and Fischer, R. (2005) The *Aspergillus nidulans* phytochrome FphA represses sexual development in red light. *Current Biology*, **15**, 1833–1838.

Borneman, A.R., Hynes, M.J. and Andrianopoulos, A. (2000) The *abaA* homologue of *Penicillium marneffei* participates in two developmental programmes: conidiation and dimorphic growth. *Molecular Microbiology*, **38**, 1034–1047.

Boyce, K.J. and Andrianopoulos, A. (2015) Fungal dimorphism: the switch from hyphae to yeast is a specialized morphogenetic adaptation allowing colonization of a host. *FEMS Microbiology Reviews*, **39**, 797–811.

Boylan, M.T. and Quail, P.H. (1991) Phytochrome a overexpression inhibits hypocotyl elongation in transgenic Arabidopsis. *Proceedings of the National Academy of Sciences of the United States of America*, **88**, 10806–10810.

Brandt, S., von Stetten, D., Günther, M., Hildebrandt, P. and Frankenberg-Dinkel, N. (2008) The fungal phytochrome FphA from *Aspergillus nidulans*. *Journal of Biological Chemistry*, **283**, 34605–34614.

Casal, J.J. and Qüesta, J.I. (2018) Light and temperature cues: multitasking receptors and transcriptional integrators. *New Phytologist*, **217**, 1029–1034.

Dunlap, J.C. and Loros, J.J. (2017) Making time: conservation of biological clocks from fungi to animals. *Microbiology Spectrum*, **5**, FUNK-0039-2016.

Engelberg, D., Perlman, R. and Levitzki, A. (2014) Transmembrane signaling in *Saccharomyces cerevisiae* as a model for signaling in metazoans: state of the art after 25 years. *Cellular Signalling*, **26**, 2865–2878.

Erwig, L.P. and Gow, N.A. (2016) Interactions of fungal pathogens with phagocytes. *Nature Reviews Microbiology*, **14**, 163–176.

Esquivel-Naranjo, E.U., Garcia-Esquivel, M., Medina-Castellanos, E., Correa-Perez, V.A., Parra-Arriaga, J.L., Landeros-Jaime, F., *et al*. (2016) A *Trichoderma atroviride* stress-activated MAPK pathway integrates stress and light signals. *Molecular Microbiology*, **100**, 860–876.

Fischer, R., Aguirre, J., Herrera-Estrella, A. and Corrochano, L.M. (2016) The complexity of fungal vision. *Microbiology Spectrum*, **4**, 1–22.

Froehlich, A.C., Noh, B., Vierstra, R.D., Loros, J. and Dunlap, J.C. (2005) Genetic and molecular analysis of phytochromes from the filamentous fungus *Neurospora crassa*. *Eukaryotic Cell*, **4**, 2140–2152.

Fujii, Y., Tanaka, H., Konno, N., Ogasawara, Y., Hamashima, N., Tamura, S., *et al*. (2017) Phototropin perceives temperature based on the lifetime of its photoactivated state. *Proceedings of the National Academy of Sciences of the United States of America*, **114**, 9206–9211.

Fuller, K.K., Loros, J.J. and Dunlap, J.C. (2015) Fungal photobiology: visible light as a signal for stress, space and time. *Current Genetics*, **61**, 275–288.

Furukawa, K., Katsuno, Y., Urao, T., Yabe, T., Yamada-Okabe, T., Yamada-Okabe, H., *et al*. (2002) Isolation and functional analysis of a gene, *tcsB,* encoding a transmembrane hybrid-type histidine kinase from *Aspergillus nidulans*. *Applied and Environment Microbiology*, **68**, 5304–5310.

Gomez-Pastor, R., Burchfiel, E.T. and Thiele, D.J. (2018) Regulation of heat shock transcription factors and their roles in physiology and disease. *Nature Reviews Molecular Cell Biology*, **19**, 4–19.

Hedtke, M., Rauscher, S., Röhrig, J., Rodriguez-Romvero, J., Yu, Z. and Fischer, R. (2015) Light-dependent gene activation in *Aspergillus nidulans* is strictly dependent on phytochrome and involves the interplay of phytochrome and white collar-regulated histone H3 acetylation. *Molecular Microbiology*, **97**, 733–745.

Herr, A. and Fischer, R. (2014) Improvement of *Aspergillus nidulans* penicillin production by targeting AcvA to peroxisomes. *Metabolic Engineering*, **25**, 131–139.

Igbalajobi, O., Yu, Z. and Fischer, R. (2019) Red- and blue-light sensing in the plant pathogen *Alternaria alternata* depends on phytochrome and the white-collar protein LreA. *mBio*, **10**, e00371–e00319.

Ji, Y., Yang, F., Ma, D., Zhang, J., Wan, Z., Liu, W. and Li, R. (2012) HOG-MAPK signaling regulates the adaptive responses of *Aspergillus fumigatus* to thermal stress and other related stress. *Mycopathologia*, **174**, 273–282.

Jung, J.H., Domijan, M., Klose, C., Biswas, S., Ezer, D., Gao, M., *et al*. (2016) Phytochromes function as thermosensors in Arabidopsis. *Science*, **354**, 886–889.

Käfer, E. (1977) Meiotic and mitotic recombination in *Aspergillus* and its chromosomal aberrations. *Advances in Genetics*, **19**, 33–131.

Kim, P.W., Rockwell, N.C., Martin, S.S., Lagarias, J.C. and Larsen, D.S. (2014) Dynamic inhomogeneity in the photodynamics of cyanobacterial phytochrome Cph1. *Biochemistry*, **53**, 2818–2826.

Lamparter, T., Michael, N., Caspani, O., Miyata, T., Shirai, K. and Inomata, K. (2003) Biliverdin binds covalently to agrobacterium phytochrome Agp1 via its ring A vinyl side chain. *Journal of Biological Chemistry*, **278**, 33786–33792.

Legris, M., Klose, C., Burgie, E.S., Rojas, C.C., Neme, M., Hiltbrunner, A., *et al*. (2016) Phytochrome B integrates light and temperature signals in Arabidopsis. *Science*, **354**, 897–900.

Liang, S.H., Cheng, J.H., Deng, F.S., Tsai, P.A. and Lin, C.H. (2014) A novel function for Hog1 stress-activated protein kinase in controlling white-opaque switching and mating in *Candida albicans*. *Eukaryotic Cell*, **13**, 1557–1566.

Lind, A.L., Smith, T.D., Saterlee, T., Calvo, A.M. and Rokas, A. (2016) Regulation of secondary metabolism by the velvet complex is temperature-responsive in Aspergillus. *G3 (Bethesda)*, **6**, 4023–4033.

Loh, E., Righetti, F., Eichner, H., Twittenhoff, C. and Narberhaus, F. (2018) RNA thermometers in bacterial pathogens. *Microbiology Spectrum*, **6**, RWR-0012-2017.

Nemecek, J.C., Wüthrich, M. and Klein, B.S. (2006) Global control of diorphism and virulence in fungi. *Science*, **312**, 583–588.

Njimona, I., Yang, R. and Lamparter, T. (2014) Temperature effects on bacterial phytochrome. *PLoS ONE*, **9**, e109794.

O'Meara, T.R. and Cowen, L.E. (2014) Hsp90-dependent regulatory circuitry controlling temperature-dependent fungal development and virulence. *Cellular Microbiology*, **16**, 473–481.

Park, Y.J. and Park, C.M. (2019) Physicochemical modeling of the phytochrome-mediated photothermal sensing. *Scientific Reports*, **9**, 10485.

Purschwitz, J., Müller, S., Kastner, C., Schöser, M., Haas, H., Espeso, E.A., *et al*. (2008) Functional and physical interaction of blue and red-light sensors in *Aspergillus nidulans*. *Current Biology*, **18**, 255–259.

Purschwitz, J., Müller, S. and Fischer, R. (2009) Mapping the interaction sites of *Aspergillus nidulans* phytochrome FphA with the global regulator VeA and the white collar protein LreB. *Molecular Genetics and Genomics*, **281**, 35–42.

Qiu, Y., Li, M., Kim, R.J., Moore, C.M. and Chen, M. (2019) Daytime temperature is sensed by phytochrome B in Arabidopsis through a transcriptional activator HEMERA. *Nature Communications*, **10**, 140.

Rockwell, N. and Lagarias, J. (2017) Phytochrome diversification in cyanobacteria and eukaryotic algae. *Current Opinion in Plant Biology*, **37**, 87–93.

Rodriguez-Romero, J., Hedtke, M., Kastner, C., Müller, S. and Fischer, R. (2010) Fungi, hidden in soil or up in the air: light makes a difference. *Annual Review of Microbiology*, **64**, 585–610.

Ruger-Herreros, C., Rodriguez-Romero, J., Fernandez-Barranco, R., Olmedo, M., Fischer, R., Corrochano, L.M. and Canovas, D. (2011) Regulation of conidiation by light in *Aspergillus nidulans*. *Genetics*, **188**, 809–822.

Sakamoto, T. and Kimura, S. (2018) Plant temperature sensors. *Sensors (Basel)*, **18**, 4365.

Schumacher, J. (2017) How light affects the life of Botrytis. *Fungal Genetics and Biology*, **106**, 26–41.

da Silva Dantas, A., Lee, K.K., Raziunaite, I., Schaefer, K., Wagener, J., Yadav, B. and Gow, N.A. (2016) Cell biology of *Candida albicans*-host interactions. *Current Opinion in Microbiology*, **34**, 111–118.

van de Veerdonk, F.L., Gresnigt, M.S., Romani, L., Netea, M.G. and Latgé, J.P. (2017) *Aspergillus fumigatus* morphology and dynamic host interactions. *Nature Reviews Microbiology*, **15**, 661–674.

Vienken, K. and Fischer, R. (2006) The $Zn(II)_2Cys_6$ putative transcription factor NosA controls fruiting body formation in *Aspergillus nidulans*. *Molecular Microbiology*, **61**, 544–554.

Wagner, D., Tepperman, J.M. and Quail, P.H. (1991) Overexpression of phytochrome B induces a short hypocotyl phenotype in transgenic Arabidopsis. *The Plant Cell*, **3**, 1275–1288.

Wang, Z., Li, N., Li, J., Dunlap, J.C., Trail, F. and Townsend, J.P. (2016) The fast-evolving phy-2 gene modulates sexual development in response to light in the model fungus *Neurospora crassa*. *mBio*, **7**, e02148.

Wenderoth, M., Garganese, F., Schmidt-Heydt, M., Soukup, S.T., Ippolito, A., Sanzani, S.M. and Fischer, R. (2019) Alternariol as virulence and colonization factor of *Alternaria alternata* during plant infection. *Molecular Microbiology*, **112**, 131–146.

Winkler, A., Arkind, C., Mattison, C.P., Burkholder, A., Knoche, K. and Ota, I. (2002) Heat stress activates the yeast high-osmolarity glycerol mitogen-activated protein kinase pathway, and protein tyrosine phosphatases are essential under heat stress. *Eukaryotic Cell*, **1**, 163–173.

Yu, Z. and Fischer, R. (2019) Light sensing and responses in fungi. *Nature Reviews Microbiology*, **17**, 25–36.

Yu, Z., Armant, O. and Fischer, R. (2016) Fungi use the SakA (HogA) pathway for phytochrome-dependent light signaling. *Nature Microbiology*, **1**, 16019.

Zienicke, B., Molina, I., Glenz, R., Singer, P., Ehmer, D., Escobar, F.V., *et al*. (2013) Unusual spectral properties of bacteriophytochrome Agp2 result from a deprotonation of the chromophore in the red-absorbing form Pr. *Journal of Biological Chemistry*, **288**, 31738–31751.

Supporting Information

Additional supporting information may be found online in the Supporting Information section at the end of the article.